REPRODUCTION OF A PLANE-WAVE SOUND FIELD USING PLANAR AND LINEAR ARRAYS OF LOUDSPEAKERS

Jens Ahrens and Sascha Spors

Deutsche Telekom Laboratories, Berlin University of Technology,
Ernst-Reuter-Platz 7, 10587 Berlin, Germany
{jens.ahrens,sascha.spors}@telekom.de

ABSTRACT

In this paper, we consider the physical reproduction of plane-wave sound fields via continuous planar respectively linear distributions of secondary point sources. Our approach employs a formulation of the reproduction equation in the spatial frequency domain to explicitly solve it for the appropriate secondary source driving signals. This constitutes a generalization of the Ambisonics approach which is typically formulated for spherical and circular secondary source arrangements. For planar arrays, the alternative formulation provided by the Kirchhoff-Helmholtz integral equation is equivalent. For linear arrays, the Kirchhoff-Helmholtz formulation appears as a far-field/high-frequency approximation of the presented approach.

Index Terms— Spatial audio, higher order Ambisonics, wave field synthesis, audio reproduction in a plane

I. INTRODUCTION

Since several decades, the problem of physically recreating a given wave field has been addressed in the audio community. It turned out that two alternative approaches exist. The first of these approaches bases on the straight-forward solution of the reproduction equation for the loudspeaker driving signals. The alternative is a technique based on the Kirchhoff-Helmholtz integral equation.

The best-known representative of the former is Ambisonics [1]. More recent formulations of Ambisonics [2] include other representatives of this technique (mainly [3], [4], [5]). The difference between the above mentioned proposals is mainly the numerical algorithm which solves the employed equation system. However, we are aware that this is a disputable question.

The alternative is known as wave-field synthesis (WFS), e.g. [6]. It employs a modified formulation of the Kirchhoff-Helmholtz integral to determine the loudspeaker driving signals. Numerous attempts of comparing the two alternatives have been made during the years. However, the results are rather unsatisfying, mostly due to the fact that Ambisonics and its relatives rely on a discrete formulation, wave field synthesis on a continuous one.

Some of the above mentioned approaches of the first type, especially [3] and [4], are principally not limited to specific loudspeaker setups. However, their formulation does not exploit any a priori knowledge of the actual loudspeaker setup giving away the potential to reduce computational complexity. The computational complexity is generally very high in [2]-[5] due to the numerical algorithms employed.

In this paper, we present a framework to sound field synthesis employing continuous planar respectively linear loudspeaker distributions. We provide analytical expressions for the loudspeaker driving signals and for the actual reproduced wave fields. We furthermore highlight the relations of the presented approach to WFS and Ambisonics. The discussion of consequences of sampling and spatial truncation of the secondary source distributions as occurring in real-world implementations is beyond the scope of this study.

Nomenclature

The following notational conventions are used: For scalar variables, lower case denotes the time domain, upper case the temporal frequency domain. The spatial frequency domain is indicated by a tilde over the respective symbol. The dependent variables of a given quantity in the spatial frequency domain indicate with respect to which dimension the spatial frequency domain is considered. Vectors are denoted by lower case boldface. The three-dimensional position vector in Cartesian coordinates is given as $\mathbf{x} = [x\ y\ z]^T$. Confer also to figure 1. The acoustic wavenumber is denoted by k. It is related to the temporal frequency by $k^2 = \left(\frac{\omega}{c}\right)^2$ with ω being the radial frequency and c the speed of sound.

Outgoing monochromatic plane and spherical waves are denoted by $e^{-j\mathbf{k}_{\text{pw}}^T\mathbf{x}}$ and $e^{-jk|\mathbf{x}|}$ respectively, with $\mathbf{k}_{\text{pw}}^T = [k_{\text{pw},x}\ \ k_{\text{pw},y}\ \ k_{\text{pw},z}] = k_{\text{pw}} \cdot [\cos\theta_{\text{pw}} \sin\phi_{\text{pw}}\ \ \sin\theta_{\text{pw}} \sin\phi_{\text{pw}}\ \ \cos\phi_{\text{pw}}]$ and $(\theta_{\text{pw}}, \phi_{\text{pw}})$ being the propagation direction of the plane wave. j is the imaginary unit. We refer to secondary sources rather than to loudspeakers since we assume their distributions to be continuous.

II. DERIVATION OF THE SECONDARY SOURCE DRIVING FUNCTIONS

In order to analyze the properties of the wave field reproduced by planar and linear secondary source distributions,

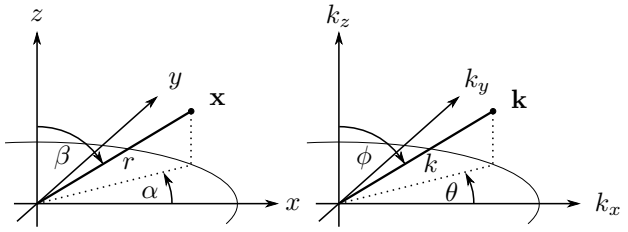

(a) Spatial domain. (b) Wave number domain.

Fig. 1. The coordinate systems used in this paper.

we have to find the appropriate secondary source driving signals. In this section, we demonstrate the derivation of the driving functions to reproduce a given monochromatic plane wave. The choice of reproducing a plane wave is justified by the fact that a suitable superposition of plane waves can be used to represent arbitrary wave fields [7].

II-A. Continuous planar secondary source arrays

The wave field reproduced by a distribution of secondary sources continuously distributed on the x-z-plane (cf. to figure 1) is given by

$$P(\mathbf{x},\omega) = \iint_{-\infty}^{\infty} D(\mathbf{x}_0,\omega)\cdot G(\mathbf{x}-\mathbf{x}_0,\omega)\; dx_0 dz_0 \;, \quad (1)$$

whereby $\mathbf{x}_0 = [x_0\ 0\ z_0]^T$ denotes the position of the secondary source driven by the signal $D(\mathbf{x}_0,\omega)$. $G(\mathbf{x}-\mathbf{x}_0,\omega)$ denotes the spatial transfer function of the secondary source located at $\mathbf{x}_0$, i.e. the spectrum of the sound field it emits when it is fed by a temporal impulse.

Before solving equation (1) for the secondary source driving signal, we have to note that we cannot expect to be able to reproduce arbitrary plane waves. Due to the omnidirectional directivity of the secondary sources the created wave field will be symmetric with respect to the secondary source distribution. The given secondary source setup will only be capable of creating wave fronts that propagate away from it. We consider this constraint by replacing the positional coordinate y with $|y|$ and indicate the replacement by subscripting a given position dependent quantity with $|y|$, e.g. $G_{|y|}$. Such a function $G_{|y|}$ then exhibits the property $G_{|y|}(x,y,z) = G_{|y|}(x,-y,z) = G_{|y|}(x,|y|,z)$.

Equation (1) essentially constitutes a two-dimensional convolution along the spatial dimensions x and z respectively. It can thus be formulated as a multiplication in the spatial frequency domain as

$$\tilde{P}_{|y|}(k_x,y,k_z,\omega) = \tilde{D}(k_x,k_z,\omega)\cdot\tilde{G}_{|y|}(k_x,y,k_z,\omega)\;. \quad (2)$$

Note that unlike [7], we assume a positive exponent for the spatial Fourier transform (cf. also to the appendix). The driving function $\tilde{D}(k_x,k_z,\omega)$ can be yielded as

$$\tilde{D}(k_x,k_z,\omega) = \frac{\tilde{P}_{|y|}(k_x,y,k_z,\omega)}{\tilde{G}_{|y|}(k_x,y,k_z,\omega)}\;. \quad (3)$$

The explicit expressions for $\tilde{P}_{|y|}(k_x,y,k_z,\omega)$ and $\tilde{G}_{|y|}(k_x,y,k_z,\omega)$ are derived in the appendix and are given by (27) and (33) respectively. Due to the constrained validity of the involved transformations the following equations are only valid for $k_{\mathrm{pw},y} > 0$ (cf. also to the appendix).

Inserting equations (27) and (33) into (3) and exploiting the sifting property of the delta function [8] yields

$$\tilde{D}(k_x,k_z,\omega) = 8\pi^2 j k_{\mathrm{pw},y}\cdot\delta(k_x-k_{\mathrm{pw},x})\;\delta(k_z-k_{\mathrm{pw},z})\times \\ \times\, 2\pi\delta(\omega-\omega_{\mathrm{pw}})\;. \quad (4)$$

Therefore,

$$D(x,z,\omega) = 2jk_{\mathrm{pw},y}\cdot e^{-jk_{\mathrm{pw},x}x}\; e^{-jk_{\mathrm{pw},z}z}\times \\ \times\, 2\pi\delta(\omega-\omega_{\mathrm{pw}})\;. \quad (5)$$

In the time domain, the exponential terms correspond to delays [7]. Thus, the driving signal for a secondary source at location $\mathbf{x}_0 = [x_0\ 0\ z_0]^T$ is yielded by a frequency dependent weighting of the time domain input signal and a delay dependent on the location of the secondary source.

II-B. Continuous linear secondary source arrays

Despite the simple driving function for the planar secondary source array, this setup will be rarely implemented due to the enormous amount of loudspeakers necessary. Typically, audio rendering systems employ linear arrays. For convenience, the secondary source array is assumed to be along the x-axis (thus $\mathbf{x}_0 = [x_0\ 0\ 0]^T$).

For this setup the analogous to the reproduction equation for planar arrays (1) reads

$$P_{|y|}(\mathbf{x},\omega) = \int_{-\infty}^{\infty} D(\mathbf{x}_0,\omega)\cdot G_{|y|}(\mathbf{x}-\mathbf{x}_0,\omega)\; dx_0\;, \quad (6)$$

respectively

$$\tilde{P}_{|y|}(k_x,y,z,\omega) = \tilde{D}(k_x,\omega)\cdot\tilde{G}_{|y|}(k_x,y,z,\omega)\;, \quad (7)$$

and finally

$$\tilde{D}(k_x,\omega) = \frac{\tilde{P}_{|y|}(k_x,y,k_z,\omega)}{\tilde{G}_{|y|}(k_x,y,z,\omega)}\;. \quad (8)$$

$\tilde{P}_{|y|}(k_x,y,k_z\omega)$ and $\tilde{G}_{|y|}(k_x,y,z,\omega)$ are given by (26) and (31). Again, the following equations are only valid for $k_{\mathrm{pw},y} > 0$ (cf. to the appendix).

Inserting (26) and (31) into (8) yields

$$\tilde{D}(k_x,\omega) = \frac{2\pi\delta(k_x-k_{\mathrm{pw},x})e^{-jk_{\mathrm{pw},y}|y|}e^{-jk_{\mathrm{pw},z}z}}{-\frac{j}{4}H_0^{(2)}\left(\sqrt{|y|^2+z^2}\sqrt{\left(\frac{\omega_{\mathrm{pw}}}{c}\right)^2-k_x^{\,2}}\right)}\times \\ \times\, 2\pi\delta(\omega-\omega_{\mathrm{pw}})\;. \quad (9)$$

We find that $|y|$ and z are apparent in the expression for the driving function suggesting that equation (6) can only be

satisfied for positions on the surface of a cylinder determined by $r = \sqrt{|y|^2 + z^2}$. However, if also the propagating direction of the plane wave is considered, it turns out that equation (6) can only be satisfied for positions on two infinite lines of listening positions parallel to the x-axis opposite of each other. In spherical coordinates, these two lines are determined by $r = \sqrt{|y|^2 + z^2}$, $\alpha = \pm\theta_{\text{pw}}$, $\beta = \phi_{\text{pw}}$. This finding is in analogy to the reproduction of a plane wave by a circular arrangement of secondary point sources where the reproduced wave field has to be referenced to a point [9]. For convenience, we want to reference the reproduction to the horizontal plane where we assume the listener's ears, thus $z \stackrel{!}{=} 0$. We consequently also have to limit the propagation directions of the desired plane wave to the horizontal plane ($\phi_{\text{pw}} \stackrel{!}{=} \frac{\pi}{2}$). We set $|y|$ to the desired distance $y_{\text{ref}} > 0$ from the secondary source array where we want the wave field to be correct. This referencing is discussed in more detail in section III-B. Note that equation (9) provides the potential to compensate for artefacts in listening positions off the target plane.

With the above mentioned referencing, equation (9) simplifies to

$$\tilde{D}(k_x, \omega) = \frac{4j \cdot e^{-jk_{\text{pw},y} y_{\text{ref}}}}{H_0^{(2)}\left(k_{\text{pw},y} y_{\text{ref}}\right)} \cdot 2\pi\delta(k_x - k_{\text{pw},x}) \times \\ \times 2\pi\delta(\omega - \omega_{\text{pw}}) \ , \quad (10)$$

and finally

$$D(x, \omega) = \frac{4j \cdot e^{-jk_{\text{pw},y} y_{\text{ref}}}}{H_0^{(2)}\left(k_{\text{pw},y} y_{\text{ref}}\right)} \cdot e^{-jk_{\text{pw},x} x} \times \\ \times 2\pi\delta(\omega - \omega_{\text{pw}}) \ . \quad (11)$$

Analogously to the case of planar secondary source distributions, the time domain secondary source driving signal can be yielded by delaying and weighting the time domain input signal. The weight is dependent on the frequency and the reference distance, the delay is dependent on the position of the respective secondary source and the reference distance. This constitutes a computationally efficient implementation scheme compared to the numerical approaches in [2]-[5].

III. REPRODUCED WAVE FIELDS

III-A. Planar secondary source arrays

The wave field reproduced by a planar secondary distribution driven according to equation (5) is yielded by inserting (5) into (1). To solve the integrals one has to substitute $u = x_0 - x$ and $v = z_0 - z$ and follow the procedure outlined in the appendix. One arrives then at equation (25) proofing perfect reproduction.

III-B. Linear secondary source arrays

Inserting equation (11) into (6) yields the wave field reproduced by an appropriately driven linear secondary source distribution. Solving the integral as indicated in section III-A yields

$$P_{\text{pw}}(\mathbf{x}, \omega) = \frac{e^{-jk_y y_{\text{ref}}}}{H_0^{(2)}(k_y y_{\text{ref}})} \cdot e^{-jk_x x} H_0^{(2)}(k_y |y|) \ . \quad (12)$$

For $|y| = y_{\text{ref}}$ equation (12) exactly corresponds to the desired wave field. However, for $|y| \neq y_{\text{ref}}$ the reproduced wave field departs from the desired one. The arising artefacts are easily identified when the far-field/high-frequency region is considered ($k_y y_{\text{ref}} \gg 1$, $k_y |y| \gg 1$). There, the Hankel functions apparent in equation (12) can be replaced by their large argument approximation $H_\nu^{(2)}(z) = \sqrt{\frac{2}{\pi z}} e^{-j(z - \nu\frac{\pi}{2} - \frac{\pi}{4})}$ [7]. The approximated reproduced wave field reads then

$$P_{\text{appr, pw}}(\mathbf{x}, \omega) = \sqrt{\frac{y_{\text{ref}}}{|y|}} e^{-jk_x x} e^{-jk_y |y|} \ . \quad (13)$$

Thus, in the far-field/high-frequency region the amplitude of the reproduced wave field $P(\mathbf{x}, \omega)$ shows a decay proportional to $\frac{1}{\sqrt{|y|}}$, i.e. approximately 3 dB with each doubling of the distance to the secondary source array. In the near-field/low-frequency region the amplitude decay is slightly different and additionally, some subtle spectral deviations are apparent. These findings have also been derived by the authors in [9] for the reproduction of a plane wave with a circular secondary point source distribution. Confer also to figures 2 and 3. Figure 2 depicts the real part and the absolute value of the sound pressure of a continuous linear distribution of secondary point sources reproducing a virtual plane wave of $f_{\text{pw}} = 1000$ Hz and unit amplitude with propagation direction $\theta_{\text{pw}} = \frac{1}{4}\pi$ referenced to the distance $y_{\text{ref}} = 1.0$ m. Figure 3 shows a cross section through $|P_{\text{pw}}(\mathbf{x}, \omega)|$ and $|P_{\text{appr, pw}}(\mathbf{x}, \omega)|$ along the y-axis. For a frequency of 1000 Hz, the approximation $P_{\text{appr, pw}}(\mathbf{x}, \omega)$ is very accurate. For lower frequencies, more obvious deviations arise close to the secondary source array. However, the amplitude deviation stays rather small. The arising phase errors are slightly more significant.

The exact formulation of the driving function, equation (11), allows for referencing also in the proximity of the secondary source array. The thorough investigation of this procedure is beyond the scope of this paper and is subject to ongoing research.

IV. RELATION TO HIGHER ORDER AMBISONICS

In this section, we highlight the relation of the presented approach to what is known as higher order Ambisonics.

In the traditional Ambisonics approach, the loudspeakers of the respective reproduction system are located on a sphere respectively on a circle around the listening area. Both the desired wave field as well as the wave fields emitted by the loudspeakers are expanded into series of orthogonal basis functions [1], [2]. The term 'higher order' simply emphasizes the fact that the expansions are not restricted to

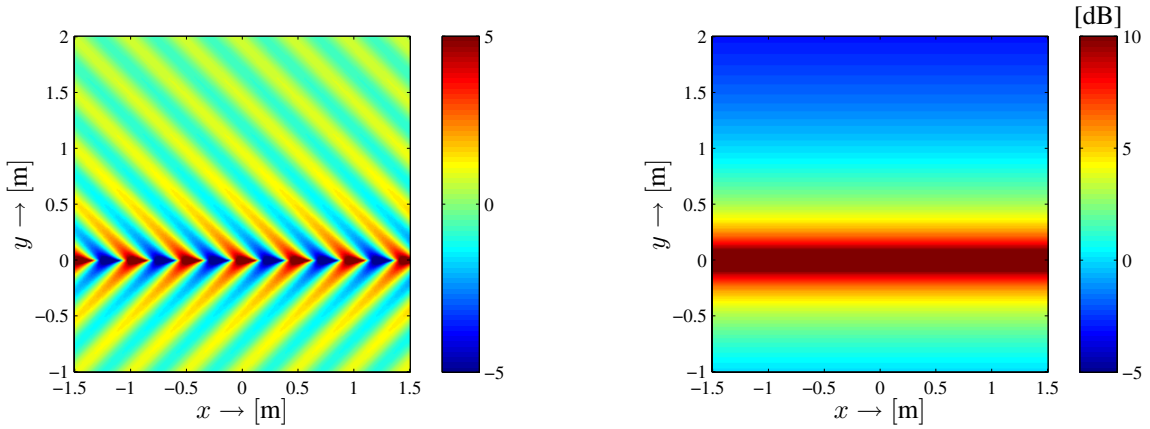

(a) $\Re\{P_{\text{pw}}(\mathbf{x}, \omega)\}$ (b) $20 \cdot \log_{10} |P_{\text{pw}}(\mathbf{x}, \omega)|$

Fig. 2. Sound pressure $P_{\text{pw}}(\mathbf{x}, \omega)$ of a continuous linear distribution of secondary point sources reproducing a virtual plane wave of $f_{\text{pw}} = 1000$ Hz and unit amplitude with propagation direction $\theta_{\text{pw}} = \frac{1}{4}\pi$ referenced to the distance $y_{\text{ref}} = 1.0$ m. The values are clipped as indicated by the colorbars.

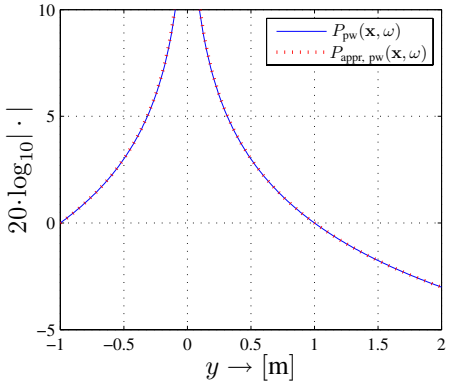

Fig. 3. Cross section through figure 2(b) along the y-axis. The far-field/high-frequency approximation $P_{\text{appr,pw}}(\mathbf{x}, \omega)$ of $P_{\text{pw}}(\mathbf{x}, \omega)$ is also indicated.

low expansion orders. This results in an equation system that is solved for the optimal loudspeaker driving signals. These drive the loudspeakers such that their superposed wave fields best approximate the desired one in a given sense:

$$P(\mathbf{x}, \omega) = \sum_{n=0}^{N-1} D(\mathbf{x}_n, r_0, \omega) \cdot G(\mathbf{x} - \mathbf{x}_n, \omega) \,, \qquad (14)$$

where $P(\mathbf{x}, \omega)$ denotes the desired wave field, $D(\mathbf{x}_n, r_0, \omega)$ the driving signal of the loudspeaker located at the position $\mathbf{x}_n = r_0 \cdot [\cos\alpha_n \sin\beta_n \;\; \sin\alpha_n \sin\beta_n \;\; \cos\beta_n]^T$, and $G(\mathbf{x} - \mathbf{x}_n, \omega)$ its spatial transfer function.

The solution of the resulting equation system is typically accomplished numerically. An analytical solution was recently presented by the authors [9]. However, the formulations are restricted to spherical/circular secondary source arrangements. The approach presented in this paper can be seen as an extension to Ambisonics allowing for the treatment of planar/linear arrangements. While equation (14) constitutes a spherical respectively circular convolution, equations (1) and (6) constitute linear ones. The Fourier transform which is applied in the presented approach to find the appropriate secondary source driving function is essentially the analog to the orthogonal expansions applied in traditional Ambisonics.

V. COMPARISON TO THE KIRCHHOFF-HELMHOLTZ FORMULATION

In this section, we compare the above derived findings to the alternative formulation given by the Kirchhoff-Helmholtz integral [7]. The Kirchhoff-Helmholtz integral states that an acoustic wave field inside a source-free volume is entirely determined by the sound pressure and sound pressure gradient distribution on the boundary of that volume enclosing it. However, in the present case we do not treat enclosed volumes but infinitely extended boundaries. We furthermore exclusively treat the sound pressure of the virtual wave field and not its gradient.

In the context of wave field synthesis (WFS), the Kirchhoff-Helmholtz formulation has been modified in exactly these terms [6], [10]:

In WFS the sound pressure inside a closed volume (or in a half space) is controlled by a continuous distribution of monopole point sources on the boundary of that volume (or in the plane dividing space into two half spaces). These modifications enable a direct comparison of the approach presented in this paper to the alternative formulation as discussed below.

V-A. Planar secondary source distributions

Although we are not aware of the existence of a three-dimensional implementation of WFS we treat it theoretically for completeness.

The modified formulation of the Kirchhoff-Helmholtz integral for planar secondary source arrays in the x-z-plane

$$P(\mathbf{x},\omega) = \iint_{-\infty}^{\infty} \underbrace{-2\frac{\partial}{\partial \mathbf{n}} S(\mathbf{x}_0,\omega)}_{D_{\text{WFS,3D}}(\mathbf{x}_0,\omega)} \cdot G_{\text{3D}}(\mathbf{x}-\mathbf{x}_0,\omega)\; dx_0 dz_0 \tag{15}$$

states that the sound pressure in the half spaces defined by the secondary source array is determined by an integration over all secondary sources driven by the driving signals $D_{\text{WFS,3D}}(\mathbf{x}_0,\omega)$. The driving signals $D_{\text{WFS,3D}}(\mathbf{x}_0,\omega)$ are given as the directional gradient $\frac{\partial}{\partial \mathbf{n}}$ normal to the secondary source distribution of the desired wave field at the respective secondary source's position. As in section II, we assume the half space in positive y-direction to be the target area. Thus, the normal vector $\mathbf{n}$ points parallel to the y-axis. Note that the free-field Green's function $G_{\text{3D}}(\mathbf{x}-\mathbf{x}_0,\omega)$ apparent in equation (15) essentially corresponds to the monopole sources employed in section II [7].

Deriving the driving function for a monochromatic plane wave with angular frequency ω_{pw} propagating into the direction $(\theta_{\text{pw}}, \phi_{\text{pw}})$ as indicated in (15) yields

$$D_{\text{WFS,3D}}(\mathbf{x},\omega) = 2jk_{\text{pw},y} \cdot e^{-j\mathbf{k}_{\text{pw}}^T\mathbf{x}} \cdot 2\pi\delta(\omega-\omega_{\text{pw}}) \;. \tag{16}$$

$D_{\text{WFS,3D}}(\mathbf{x},\omega)$ evaluated at $y=0$ essentially corresponds to the driving function for our approach given by equation (5), thus proofing the equivalence of the two approaches.

V-B. Linear secondary source distributions

For linear secondary source distributions along the x-axis the WFS formulation reads

$$P(\mathbf{x},\omega) = \int_{-\infty}^{\infty} \underbrace{-2\frac{\partial}{\partial \mathbf{n}} S(\mathbf{x}_0,\omega)}_{D_{\text{WFS,2D}}(\mathbf{x}_0,\omega)} \cdot G_{\text{2D}}(\mathbf{x}-\mathbf{x}_0,\omega)\; dx_0 \;. \tag{17}$$

The driving function for a monochromatic plane wave with angular frequency ω_{pw} propagating into the direction $(\theta_{\text{pw}}, \frac{\pi}{2})$ evaluated at $y=0, z=0$ is then

$$D_{\text{WFS,2D}}(x,\omega) = 2jk_{\text{pw},y} \cdot e^{-jk_{\text{pw},x}x} \cdot 2\pi\delta(\omega-\omega_{\text{pw}}) \;. \tag{18}$$

The two-dimensional WFS equation (17) employs the two-dimensional free-field Green's function [7]

$$G_{\text{2D}}(\mathbf{x}-\mathbf{x}_0,\omega) = \frac{j}{4} H_0^{(2)}\left(\frac{\omega}{c}|\mathbf{x}-\mathbf{x}_0|\right) \tag{19}$$

which can be interpreted as the spatial transfer function of a line source. However, WFS typically employs loudspeakers with closed cabinets as secondary sources whose behavior can be better approximated by that of point sources. This secondary source mismatch has to be compensated for.

In the far-field/high-frequency region $G_{\text{2D}}(\mathbf{x}-\mathbf{x}_0,\omega)$ can be approximated as (cf. to section III-B)

$$G_{\text{2D}}(\mathbf{x}-\mathbf{x}_0,\omega) \approx \sqrt{\frac{2\pi}{j\frac{\omega}{c}}}\sqrt{|\mathbf{x}-\mathbf{x}_0|} \cdot \underbrace{\frac{1}{4\pi}\frac{e^{-j\frac{\omega}{c}|\mathbf{x}-\mathbf{x}_0|}}{|\mathbf{x}-\mathbf{x}_0|}}_{G_{\text{3D}}(\mathbf{x}-\mathbf{x}_0,\omega)} \;, \tag{20}$$

where the spatial transfer function $G_{\text{3D}}(\mathbf{x}-\mathbf{x}_0,\omega)$ of a point source is apparent (cf. to equation (29)). Thus, in the far-field/high-frequency region the secondary source mismatch can be compensated for as [10]

$$D_{\text{appr,WFS,2D}}(x,\omega) = \sqrt{\frac{2\pi}{jk_{\text{pw}}}}\sqrt{y_{\text{ref}}} \cdot D_{\text{WFS,2D}}(x,\omega) \;, \tag{21}$$

with y_{ref} denoting the reference distance. More explicitly,

$$D_{\text{appr,WFS,2D}}(x,\omega) = 2\sqrt{2\pi jk_{\text{pw},y}}\sqrt{y_{\text{ref}}} \cdot e^{-jk_{\text{pw},x}x} \times \\ \times\, 2\pi\delta(\omega-\omega_{\text{pw}}) \;. \tag{22}$$

The far-field/high-frequency approximation of the non-holographic driving function equation (11) reads

$$D_{\text{appr,2D}}(x,\omega) = 2\sqrt{2\pi jk_{\text{pw},y}}\sqrt{y_{\text{ref}}} \cdot e^{-jk_{\text{pw},x}x} \cdot 2\pi\delta(\omega-\omega_{\text{pw}}) \tag{23}$$

Thus, the two driving functions are similar when the far-field/high-frequency region is considered. However, our approach provides the capability of referencing the reproduced wave field in the near-field/low-frequency region (cf. to section III-B). WFS does not allow this.

VI. CONCLUSIONS

A unified framework for the physical reproduction of plane-wave sound fields by continuous planar and linear secondary point source arrangements was presented. For planar arrays, the desired wave field is perfectly reproduced in one of the half spaces defined by the secondary source distribution. The wave field in the other half space is equal but mirrored on the secondary source arrangement. The treatment of linear secondary source arrangements revealed that the wave field can only be perfectly reproduced on two infinite lines parallel to the secondary source distribution opposite of each other. The reproduced wave field shows an amplitude decay of approximately 3 dB with every doubling of the distance and slight spectral deviations. Plane waves propagating parallel to the secondary source arrays can not be recreated. This fact emerges in a restricted validity of the involved transformations.

Since no ambiguities arose in the derivation of the driving function for a given plane wave, the solution can be assumed to be unique. This finding is supported by the fact that the comparison to the alternative formulation provided by the Kirchhoff-Helmholtz integral showed that the two approaches are equivalent. In the case of a linear distribution, the presented approach provides the capability of referencing the reproduced wave field in the near-field/low-frequency region. Kirchhoff-Helmholtz based audio reproduction as implemented in wave field synthesis can only provide a far-field/low-frequency approximation. Note that the computational complexity is equally low for both approaches.

It was furthermore shown that the presented approach

constitutes a generalization of what is known as Ambisonics.

VII. REFERENCES

[1] M.A. Gerzon, "With-heigth sound reproduction," *Journal of the Audio Eng. Soc. (JAES)*, vol. 21, pp. 2–10, 1973.

[2] J.Daniel, "Représentation de champs acoustiques, application à la transmission et à la reproduction de scènes sonores complexes dans un contexte multimédia," PhD thesis Université Paris 6, 2001.

[3] O. Kirkeby and P.A. Nelson, "Reproduction of plane wave sound fields," *JASA 94(5)*, Nov. 1993.

[4] D.B. Ward and T.D. Abhayapala, "Reproduction of a plane-wave sound field using an array of loudspeakers," *IEEE Trans. on Sp. and Audio Proc.*, vol. 9(6), Sep. 2001.

[5] M.A. Poletti, "Three-dimensional surround sound systems based on spherical harmonics," *Journal of the Audio Eng. Soc. (JAES)*, vol. 53, no. 11, pp. 1004–1025, Nov. 2005.

[6] A.J. Berkhout, D. de Vries, and P. Vogel, "Acoustic control by wave field synthesis," *JASA 93(5)*, May 1993.

[7] E.G. Williams, *Fourier Acoustics: Sound Radiation and Nearfield Acoustic Holography*, Academic Press, London, 1999.

[8] B. Girod, R. Rabenstein, and A. Stenger, *Signals and Systems*, J.Wiley & Sons, 2001.

[9] J. Ahrens and S. Spors, "Analytical driving functions for higher order ambisonics," in *IEEE ICASSP*, Las Vegas, Nevada, March 30th–April 4th 2008.

[10] R. Rabenstein and S. Spors, "Sound field reproduction," In Benesty, J., Sondhi, M., Huang, Y, (Eds.), Springer Handbook on Speech Processing and Speech Communication, Springer Verlag, 2007.

[11] I.S. Gradshteyn and I.M. Ryzhik, *Table of Integrals, Series, and Products*, Academic Press, San Diego, 2000.

APPENDIX

FOURIER TRANSFORMS OF A PLANE WAVE

A monochromatic plane wave with angular frequency ω_{pw} and unit amplitude propagating into the direction $(\theta_{\text{pw}}, \phi_{\text{pw}})$ is described by

$$p(\mathbf{x}, t) = e^{-j\mathbf{k}_{\text{pw}}^T\mathbf{x}} \cdot e^{j\omega_{\text{pw}}t} \ . \tag{24}$$

As discussed in section II-A, the wave field described by equation (24) cannot be perfectly recreated with the secondary source setups discussed in this paper. The reproduction is constricted to $p_{|y|}(\mathbf{x}, t)$.

A Fourier transform of $p_{|y|}(\mathbf{x}, t)$ with respect to t yields [8]

$$P_{|y|}(\mathbf{x}, \omega) = e^{-j\mathbf{k}_{\text{pw}}^T\mathbf{x}} \cdot 2\pi\delta(\omega - \omega_{\text{pw}}) \ . \tag{25}$$

A further Fourier transform with respect to x yields

$$\tilde{P}_{|y|}(k_x, y, z, \omega) = 2\pi\delta(k_x - k_{\text{pw},x}) \ e^{-jk_{\text{pw},y}|y|} \ e^{-jk_{\text{pw},z}z} \times \\ \times \ 2\pi\delta(\omega - \omega_{\text{pw}}) \ , \tag{26}$$

and finally

$$\tilde{P}_{|y|}(k_x, y, k_z, \omega) = 4\pi^2\delta(k_x - k_{\text{pw},x}) \ e^{-jk_{\text{pw},y}|y|} \times \\ \times \ \delta(k_z - k_{\text{pw},z}) \cdot 2\pi\delta(\omega - \omega_{\text{pw}}) \ , \tag{27}$$

whereby $\delta(\cdot)$ denotes the Dirac delta function [8].

FOURIER TRANSFORMS OF A POINT SOURCE

The spatial transfer function of an acoustic point source situated at the coordinate origin is described by

$$g(\mathbf{x}, t) = \frac{1}{4\pi} \frac{\delta(t - \frac{|\mathbf{x}|}{c})}{|\mathbf{x}|} \ , \tag{28}$$

with $|\mathbf{x}| = \sqrt{x^2 + y^2 + z^2}$. The factor $\frac{1}{4\pi}$ was introduced for convenience to allow an interpretation of $g(\mathbf{x}, t)$ as free-field Green's function [7] (cf. to section V). We furthermore replace y^2 by $|y|^2$ in (28). This replacement is justified since $y^2 = |y|^2$. It will be of significance as discussed below.

The temporal Fourier transform of (28) is then

$$G_{|y|}(\mathbf{x}, \omega) = \frac{1}{4\pi} \frac{e^{-j\frac{\omega}{c}|\mathbf{x}|}}{|\mathbf{x}|} \ . \tag{29}$$

The Fourier transform with respect to x reads

$$\tilde{G}_{|y|}(k_x, y, z, \omega) = \frac{1}{4\pi} \int_{-\infty}^{\infty} \frac{e^{-j\frac{\omega}{c}\sqrt{x^2+|y|^2+z^2}}}{\sqrt{x^2 + |y|^2 + z^2}} e^{jk_x x} dx \ . \tag{30}$$

With [11, (3.876-1) and (3.876-2)] one yields

$$\tilde{G}_{|y|}(k_x, y, z, \omega) = -\frac{j}{4} H_0^{(2)} \left(\sqrt{|y|^2 + z^2} \sqrt{\left(\frac{\omega}{c}\right)^2 - {k_x}^2} \right) \ . \tag{31}$$

$H_0^{(2)}(\cdot)$ denotes the zeroth-order Hankel function of second kind [7]. Equation (31) is only valid for $\sqrt{k_y^2 + k_z^2} > 0$ [11].

A further Fourier transform with respect to z is

$$\tilde{G}_{|y|}(k_x, y, k_z, \omega) = \\ = -\frac{j}{4} \int_{-\infty}^{\infty} H_0^{(2)} \left(\sqrt{|y|^2 + z^2} \sqrt{\left(\frac{\omega}{c}\right)^2 - {k_x}^2} \right) e^{jk_z z} dz \ . \tag{32}$$

With [11, (6.677-3) and (6.677-4)] one finally yields

$$\tilde{G}_{|y|}(k_x, y, k_z, \omega) = -\frac{j}{2} \frac{e^{-jk_y \cdot |y|}}{k_y} \ , \tag{33}$$

whereby the relation $\sqrt{(\frac{\omega}{c})^2 - k_x^2 - k_z^2} = k_y$ has been exploited. Note that equations (31) and (33) are only valid for $k_y > 0$. By having replaced y^2 with $|y|^2$ as discussed above, we ensured the validity of (33) for all possible values of y [11].